

# Adaptive Mesh Grouping in Electrical Impedance Tomography for Bubble Visualization

Kyungho Cho\* and Sin Kim\*

(Received January 8, 1999)

The bubble visualization in two-phase flow using the EIT (Electrical Impedance Tomography) technique requires an image reconstruction process. When the conventional iterative image reconstruction algorithms are used, the processing time increases rapidly and the convergence characteristics become very poor as the spatial resolution increases. In order to overcome this problem, this study proposes an adaptive mesh grouping method utilizing the genetic algorithm and the fuzzy set theory. Computer simulations using the improved Newton-Raphson method combined with the proposed method show promising results that mesh grouping may become a useful way to mitigate the ill-conditioning phenomenon which makes the EIT inverse problem difficult.

**Key Words:** Electrical Impedance Tomography, Two Phase Flow, Bubble Visualization, Genetic Algorithm, Fuzzy Set Theory, Inverse Problem

## 1. Introduction

It is very important to understand precisely the two-phase flow phenomena in the thermal hydraulic systems. Various two-phase flow measuring techniques have been suggested and devised. Based upon their principles, they can be classified into radioactive absorption and scattering (Shollenberger, 1997), impedance (or capacitance) (Dickin, 1996; Elkow, 1996; Ovacik, 1997a and 1997b), optical (Vassallo, 1993), acoustic (Xu, 1997) technique and so on. Also these can be divided into invasive and non-invasive techniques according to whether flow fields are disturbed or not by the measuring equipments. Conductivity or optical probes are the typical intrusive ones. Conversely, as a non-intrusive technique, radiological equipments are adopted. Recently, many efforts are given to the development of optical techniques such as LDV (Laser Doppler Velocimetry) and PIV (Particle Image Velocimetry) methods. However, there still

remain open issues on these techniques that (i) the probes inserted into flow fields not only disturb the flow inevitably but also take the information only at the neighboring regions around the probes and (ii) the radiological or optical methods give rather spatially-averaged informations over the measured flow fields.

Recently, there are several researches (Cho, 1997; Dickin, 1996; Elkow, 1996; Ovacik, 1997a and 1997b) that applied the EIT (Electrical Impedance Tomography) technology (Webster, 1990; Woo, 1990) to the multi-phase flow to investigate the flow mechanism more precisely. The results, however, show that there still remain several problems to be resolved for the EIT technology to be a useful tool to measure the bubble distribution (Cho, 1997; Ovacik, 1997a and 1997b). The major difficulties come from the image reconstruction process. In the bubble visualization via the EIT, the resistivity distribution at a certain instance is reconstructed as an image for the bubble distribution at the measuring section. The image reconstruction in the EIT is characterized as a difficult inverse problem due to its high non-linearity and ill-posedness.

Using the improved Newton-Raphson method

\* Dept. of Nuclear and Energy Engineering Cheju National University, 1 Ara-Dong, Cheju 690-756, Korea.

(iNR) and the finite element method as the image reconstruction algorithm and the modeling method, respectively, it takes unbearable amount of computation time on a personal computer to reconstruct an image with 5% spatial resolution (Woo, 1993). To reduce the computational time, several researchers suggested various element or mesh grouping methods. In these methods, they forced all meshes belonging to a certain group to have the same resistivity value (Woo, 1992; Glidewell 1995; Paulsen, 1995). If meshes are appropriately grouped, the number of variables can be reduced without sacrificing the spatial resolution. This helps not only to reduce the computation time but also to improve the sensitivity problem, because the size of the grouped meshes becomes bigger than the size of a single mesh. In the above grouping methods suggested so far, however, meshes are grouped rather in pre-determined ways. So, they are very limited to some specific applications (e. g. for medical imaging) and not suitable to the bubble visualization via the EIT technology.

In two-phase flow fields, we may assume that there are only two different representative resistivity values; one resistivity value for the background (e. g. water) and the other for the target (e. g. bubbles). Thus, meshes belonging to a certain phase may have the same resistivity value. Based on this observation, this study proposes an adaptive mesh grouping method where the mesh grouping changes adaptively during the image reconstruction process based on a fuzzy-genetic algorithm for the bubble visualization in two-phase flow fields.

## 2. Iterative Image Reconstruction Method and Ill-Conditioning Problem

In this paper, we adopted iNR (Webster, 1990; Woo, 1993 and 1994) as a basic image reconstruction algorithm for the EIT. The iNR algorithm is an improved version of the modified Newton-Raphson method developed in the University of Wisconsin-Madison. Given a FEM model for the flow domain with a possible bubble distribution as shown in Fig. 1 where each mesh has its own

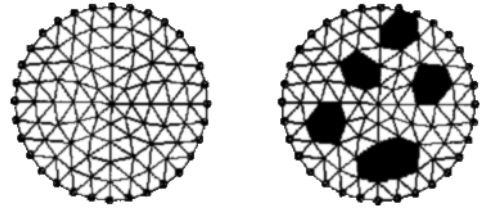


Fig. 1 FEM mesh model and bubbles.

unknown resistivity value, the iterative image reconstruction procedure can be formulated as follows.

Let the unknown resistivity distribution vector of the FEM model be  $\rho = [\rho_1, \rho_2, \dots, \rho_N]^T$  where  $\rho_i$  ( $i=1, \dots, N$ ) is the resistivity value of the  $i$ -th element. Let  $e = [e_1, e_2, \dots, e_M]^T$  be the error vector between the calculated ( $f(\rho) = [f_1(\rho), f_2(\rho), \dots, f_M(\rho)]^T$ ) and the measured ( $v = [v_1, v_2, \dots, v_M]^T$ ) voltages at  $M$  boundary nodes. Then, the image reconstruction in the EIT becomes a problem of finding  $\rho$  that minimizes the objective function defined as:

$$\phi(\rho) = \|e\| = (f(\rho) - v)^T (f(\rho) - v). \quad (1)$$

To find  $\rho$  which minimizes  $\phi(\rho)$ , we set its derivative to zero, i. e.,

$$\phi'(\rho) = [f'(\rho)]^T (f(\rho) - v) = 0 \quad (2)$$

where,  $[f'(\rho)]_{ij} = \frac{\partial f_i}{\partial \rho_j}$  called the Jacobian matrix. Taking Taylor series expansion of  $\phi'(\rho)$  about a point  $\rho^k$  and keep the linear terms

$$\phi'(\rho^{k+1}) = \phi'(\rho^k) + \phi''(\rho^k) \Delta \rho^k = 0 \quad (3)$$

$$\rho^{k+1} = \rho^k + \Delta \rho^k. \quad (4)$$

The term  $\phi''$  is called the Hessian matrix expressed as

$$\phi'' = [f']^T f' + [f'']^T (I \otimes [f - v]) \quad (5)$$

where  $\otimes$  is the Kronecker matrix product and  $f$ ,  $f'$  and  $f''$  are to be evaluated at  $\rho^k$ . We omit the second term in the above equation since  $f''$  is relatively small value and thus is difficult to be calculated accurately. Therefore, Eq. (5) will be

$$\phi'' = [f']^T f'. \quad (6)$$

Substituting Eq. (6) into Eq. (3),

$$\Delta \rho^k = -H^{-1} J^T (f - v). \quad (7)$$

Here,

$$H = \phi'' = [f']^T f' \quad \text{and} \quad J = f' \quad (8)$$

where  $f$ ,  $J$  and  $H$  are to be evaluated at  $\rho^k$ . In the iterative method, the solution  $\rho^k$  is updated by Eqs. (4) and (7) until a pre-specified stop condition is satisfied.

Since we do not know a priori which meshes belong to which phase, we start with  $N$  unknown variables i. e. the total number of the meshes. It is, of course, much greater than the actual number of the unknown resistivity values (e. g. 2 for two-phase flow). Therefore, the matrix size of Hessian  $H$  becomes unnecessarily large. Since it is known that the Hessian matrix  $H$  is very ill-conditioned for large elements, the computed  $\Delta\rho^k$  is also very sensitive to errors in the calculation of Jacobian and Hessian matrices including the measurement and finite element modeling errors. To overcome this ill-conditioning problem, several methods such as the regularization method (Hua, 1988), the singular value decomposition method (Murai and Kagawa, 1985) and the Marquardt method (Yorkey, 1986) have been presented. The maximal distinguishability (Isaacson, 1986) and the optimal current patterns (Hua, 1987) are also useful concept to overcome the ill-conditioning problem in the image reconstruction.

Even though their partial fulfillments are great in a certain numerical process, none of the aforementioned methods has succeeded in reconstructing the EIT images of practical resolution in a reasonable processing time even at the noise-free simulations. At the next section, we will introduce a new practical method which helps overcome the ill-conditioning problem in reconstructing the EIT image for the two-phase flow visualization by reducing the unknowns through an appropriate mesh grouping method.

### 3. Adaptive Mesh Grouping Based on Fuzzy-GA

#### 3.1 Basic idea of adaptive mesh grouping

One of the major problems in iNR is the rapid increase of the amount of computations and the poor convergence characteristics as the number of

unknown variables (or the number of meshes)  $N$  increases. However, even after a few iterations, an absolute values can not obtained but some useful informations on the target images like the approximate outlines of the target and so on can be obtained. So we may tentatively determine which mesh or group of meshes might belong to the target (e. g. bubble) or to the background (e. g. water).

Therefore, after a few iterations of iNR, we stop and examine the intermediate results. Then, we group all meshes whose resistivity values and changes are similar to each other. The exact meaning of this similarity will be described later in this paper (Sections 3.3 and 3.4). Mesh grouping reduces the number of unknown variables and increases the size of the effective mesh, so it helps to improve the condition number of the Hessian matrix in iNR method to solve the Eq. (1). By alternating iNR iterations and groupings repeatedly, we expect to improve the convergence characteristics as well as to reduce the image reconstruction time.

#### 3.2 Three mesh groups

In two-phase flow fields, we may assume that there are only two different representative resistivity values; one resistivity value for the background (e. g. water) and the other for the target (e. g. bubbles). Here, the target needs not be a single segment. It could be multiple segments of same resistivity value.

After a few initial iNR iterations performed without any grouping, we classify each mesh into one of three mesh groups: 'BaseGroup' is the mesh group with the resistivity value of the background. 'ObjectGroup' is the mesh group with the resistivity value of the object or the target like bubbles. 'AdjustGroup' is the group of meshes neither in BaseGroup nor in ObjectGroup. All meshes in BaseGroup and ObjectGroup are forced to have the same but unknown resistivity values, respectively. However, all meshes in AdjustGroup can have different resistivity values.

Mesh grouping is performed through two stages. At the first stage (Section 3.3), we roughly classify the mesh groups by applying the Genetic

Algorithm to the resistivity distribution from the iNR iteration just finished. At the second stage (Section 3.4), we refine and/or revise the GA's classifications, if necessary, by examining the changes of resistivity values of each mesh during the previous iNR iterations based upon the fuzzy set theory.

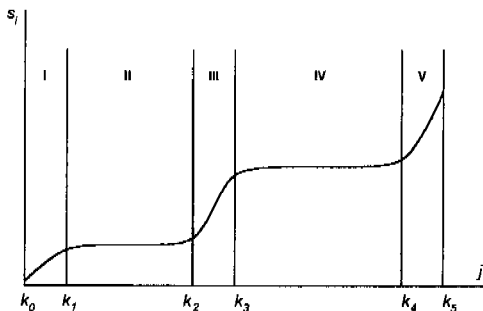
**3.3 Mesh grouping by Genetic Algorithm**

After several iNR iterations with or without any mesh grouping, we start a new mesh-grouping procedure. Firstly, we rearrange the resistivity values of meshes by sorting them in ascending order. Let  $s_j (j=1, \dots, N)$  be the resistivity distribution after this rearrangement. Then, the typical shape of  $s_j$  distribution becomes the curve shown in Fig. 2 during the reconstruction process. In Fig. 2, it is very natural to assume that meshes in regions II and IV belong to BaseGroup (water) and ObjectGroup (bubbles), respectively. All meshes in regions I, III, and V can be classified into AdjustGroup.

However, since we cannot always expect to get such a well-distinguished resistivity distribution as shown in Fig. 2, it is not trivial to divide it into the five regions properly and determine the representative resistivity for each region. Let  $\bar{\rho}_i (i=1, \dots, 5)$  be the representative resistivity value in each region and  $k_j (j=1, \dots, 4)$  be the boundary location between regions. Then, we can formulate the following optimization problem to determine  $\bar{\rho}_i$  and  $k_j$ ;

Find

$$X = \{ \bar{\rho}_1, \bar{\rho}_2, \bar{\rho}_3, \bar{\rho}_4, \bar{\rho}_5, k_1, k_2, k_3, k_4 \} \quad (9)$$



**Fig. 2** Typical distribution of the sorted resistivity values during image reconstruction.

to maximize

$$\text{fitness}(X) = \frac{1}{D} \quad (10)$$

subject to

$$D = \sum_{i=1}^5 \sum_{j=k_{i-1}}^{k_i} (s_j - \bar{\rho}_i)^2, \quad k_0=1, \quad k_5=N \quad (11)$$

where

$X$  : a candidate solution

$s_j (s_j \leq s_{j+1}, j=1, \dots, N)$  : resistivity value rearranged in ascending order,

$\bar{\rho}_i (i=1, \dots, 5)$  : representative resistivity value in each region,

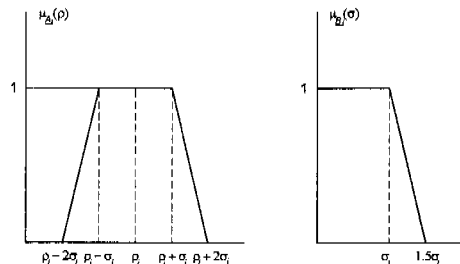
$k_j (j=1, \dots, 4)$  : boundary of regions, and

$N$  : total number of variables or meshes.

We solve the problem described in Eqs. (9) ~ (11) using the Genetic Algorithm (GA) (Goldberg, 1989) and get a solution which provides one way of dividing the regions. Then,  $\bar{\rho}_{base}$  and  $\bar{\rho}_{obj}$  are the average resistivity values of meshes in BaseGroup and ObjectGroup, respectively.  $\bar{\sigma}_{base}$  and  $\bar{\sigma}_{obj}$  are the standard deviations of resistivity values of meshes in BaseGroup and ObjectGroup, respectively.

**3.4 Fuzzy sets of meshes for background and target**

After we classified all meshes by solving the problem defined in Eqs. (9) ~ (11), we apply a fuzzy classification stage to confirm the validity of the GA's mesh classification based on the information about how the resistivity value of a single mesh has been changed during the previous iNR iterations. We impose two additional requirements on all meshes in BaseGroup and ObjectGroup so that they belong to the corresponding



**Fig. 3** Membership functions of  $\mu_{A_i}(\rho)$  and  $\mu_{B_i}(\sigma)$  ( $\rho_1 = \bar{\rho}_{base}$ ,  $\rho_2 = \bar{\rho}_{obj}$ ,  $\sigma_1 = \bar{\sigma}_{base}$ ,  $\sigma_2 = \bar{\sigma}_{obj}$ ).

groups; Firstly, in order for a mesh to belong to a mesh group, its average resistivity value during the previous iNR iterations must be within some small range from either  $\bar{\rho}_{base}$  or  $\bar{\rho}_{obj}$ . Secondly, its standard deviation of resistivity value during the same iterations must also be within some small range from either  $\bar{\sigma}_{base}$  or  $\bar{\sigma}_{obj}$ .

We now define four fuzzy sets by membership functions shown in Fig. 3 as follows:

$$\underline{A}_i = \{(\rho, \mu_{A_i}(\rho)) | \rho \in R\}, \quad i=1,2 \quad (12)$$

$$\underline{B}_i = \{(\sigma, \mu_{B_i}(\sigma)) | \sigma \in R\}, \quad i=1,2 \quad (13)$$

where,  $\underline{A}_i$  is a fuzzy set of resistivity values that can possibly belong to BaseGroup ( $i=1$ ) or ObjectGroup ( $i=2$ ) and  $\underline{B}_i$  is a fuzzy set of standard deviations of resistivity values that can possibly belong to BaseGroup ( $i=1$ ) or ObjectGroup ( $i=2$ ).

Let's define another two fuzzy sets,  $\underline{G}_i$ , as fuzzy sets of all meshes belonging to BaseGroup ( $i=1$ ) and ObjectGroup ( $i=2$ ). Then, we obtain these fuzzy sets so as to satisfy the two aforementioned requirements:

$$\underline{G}_i = \underline{A}_i \cap \underline{B}_i = \{(j, \mu_{G_i}(j)) | j=1,2,\dots,N\}, \quad i=1,2. \quad (14)$$

Here, the membership functions  $\mu_{G_i}(j)$  are determined as follows:

$$\mu_{G_i}(j) = \min\{\mu_{A_i}(\rho_j), \mu_{B_i}(\sigma_j)\}, \quad j=1,2,\dots,N. \quad (15)$$

Then, we can obtain the normal sets of meshes,  $G_{base}$  and  $G_{obj}$ , for BaseGroup and ObjectGroup by applying the  $\alpha_1$  and  $\alpha_2$  cuts of fuzzy sets  $\underline{G}_1$  and  $\underline{G}_2$ , respectively (Zimmermann, 1985):

$$G_{base} = \{j | \mu_{G_1}(j) \geq \alpha_1\}, \quad (16)$$

$$G_{obj} = \{j | \mu_{G_2}(j) \geq \alpha_2\}. \quad (17)$$

In this work, we found heuristically that the results of Eqs. (16) and (17) do not seriously depend upon the  $\alpha_1$  and  $\alpha_2$  values ranging 0.8~1. If there is any mesh that had been classified to BaseGroup (or ObjectGroup) from the solution of Eqs. (9)~(11) but turned out not to belong to  $G_{base}$  (or  $G_{obj}$ ) by Eqs. (16) and (17), we revise their grouping indices to AdjustGroup.

### 3.5 Possible grouping errors and their correction

As already noted by other researchers (Issacson, 1986; Hua, 1987), the EIT image reconstruction process is a highly nonlinear and very ill-posed inverse process. So, the grouping method proposed above does not always provide correct results. In other words, there may exist some mis-classifications in the mesh grouping because most of the informations used in the mesh grouping come from the iNR iteration results, some of which might have been contaminated seriously due to the inherent ill-posedness. It should be notified that the iNR iterations seldom converge when many meshes are mis-classified. So it is required to correct the mis-classification, if necessary.

From many observations of numerical simulations, we have found that there are three kinds of typical resistivity behavior during the iNR iterations;

- 1) Poor convergence behavior with large oscillation
- 2) Convergence behavior with small oscillation
- 3) Pseudo-convergence behavior with small oscillation

The major task in the mesh grouping is to determine which elements belong to which category among the above three behaviors. Of course, there may still remain some elements showing the first type behavior during iterations due to the ill-posed characteristics even though there is no element of the third type pseudo-convergence behavior. In case of a rather simple problem where there exists no mesh of the third type behavior, the proposed mesh grouping method works well without any mis-classification. As the problem becomes difficult, however, there appear some meshes whose resistivities undergo the third type of pseudo-convergence behavior. In this situation the mesh grouping error (or misclassification) is likely to occur at these pseudo-convergent meshes. Whenever the meshes of the third type behavior exist, we observed, there also exist concurrently some meshes undergoing the first type behavior almost near around the third

type ones. The third type behavior usually occurs at the meshes of the central area of the problem domain where the sensitivity of the boundary voltage to the resistivity of a mesh is very poor.

Actually, we have no useful measure to identify the third type meshes during the reconstruction process. In this work, however, simply and easily we can almost avoid or resolve the aforementioned mis-classification by searching the meshes of the first type behavior and by resetting the grouping indices to AdjustGroup of these meshes including their node-neighboring meshes. Here, the node-neighboring ones of a mesh mean all the elements which are connected with the mesh through its nodes.

After the mesh grouping and correction of the mis-classification if exists, we prepare a new initial guess for the subsequent iNR iterations. All the meshes belonging to BaseGroup and ObjectGroup are forced to have the new initial values of  $\bar{\rho}_{base}$  and  $\bar{\rho}_{obj}$ , respectively. For the

new initial resistivity values of the meshes in AdjustGroup, we use the average resistivity value  $\bar{\rho}_{adj}$  in this group. However, the resistivity values for AdjustGroup can change independently in the subsequent iNR iterations.

Figure 4 shows a flow chart for the mesh grouping method proposed above. As can be seen in Fig. 4, the iNR iteration and the mesh grouping repeats alternatively until we obtain a converged image. In terms of the objective function defined by Eq. (1), we decide that the reconstructed image is almost converged to the true one when the objective value  $\phi(\rho)$  is less than  $10^{-7}$ . Throughout the repeated grouping processes the BaseGroup and ObjectGroup are adaptively changed to increase and AdjustGroup size becomes smaller and smaller. Therefore, the total number of unknown variables decreases from the initial value  $N$  to the number of meshes in the reduced AdjustGroup plus one or two as the reconstruction proceeds. It will be shown in Sec. 4.2 that the

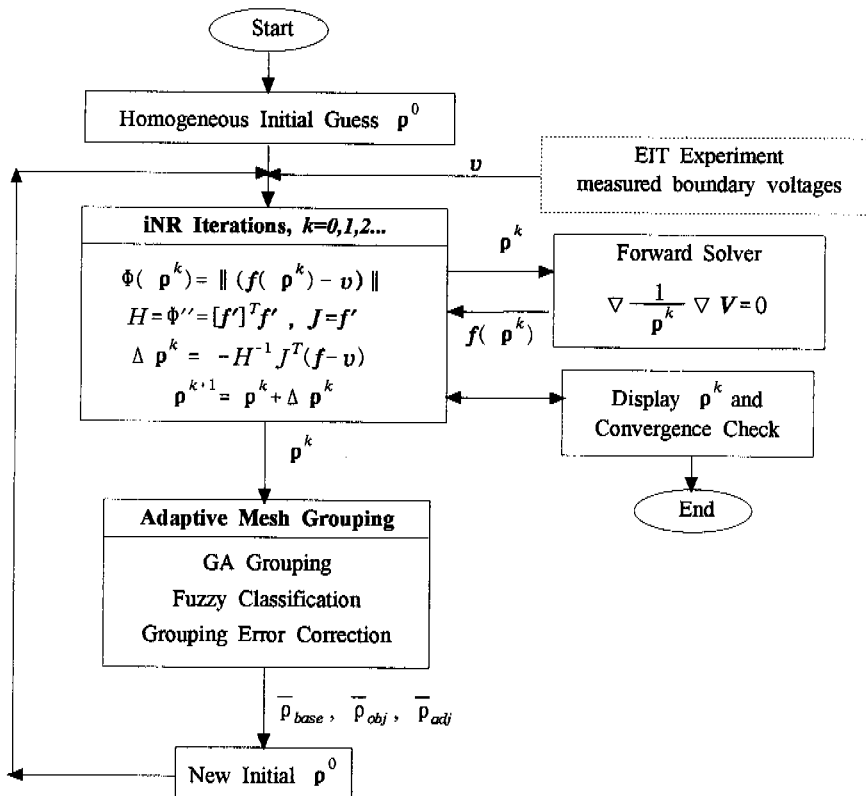


Fig. 4 Flow chart for the EIT reconstruction method using the proposed mesh grouping.

reduction of the unknown variables means not only the reduction of the computational time but also the improvement of the ill-conditioning of the system with decreased condition numbers.

#### 4. Computer Simulations and Discussions

We performed several computer simulations to compare the performance of the proposed mesh grouping method with iNR—the well-known conventional method for the future application of the bubble visualization. In the computer simulations, we assumed noise free in voltage measurement mainly for the easy comparison. We started the first iNR iterations without any mesh grouping with an arbitrary homogeneous initial guess for the resistivity distribution.

##### 4.1 Quality of reconstructed image and reconstruction time

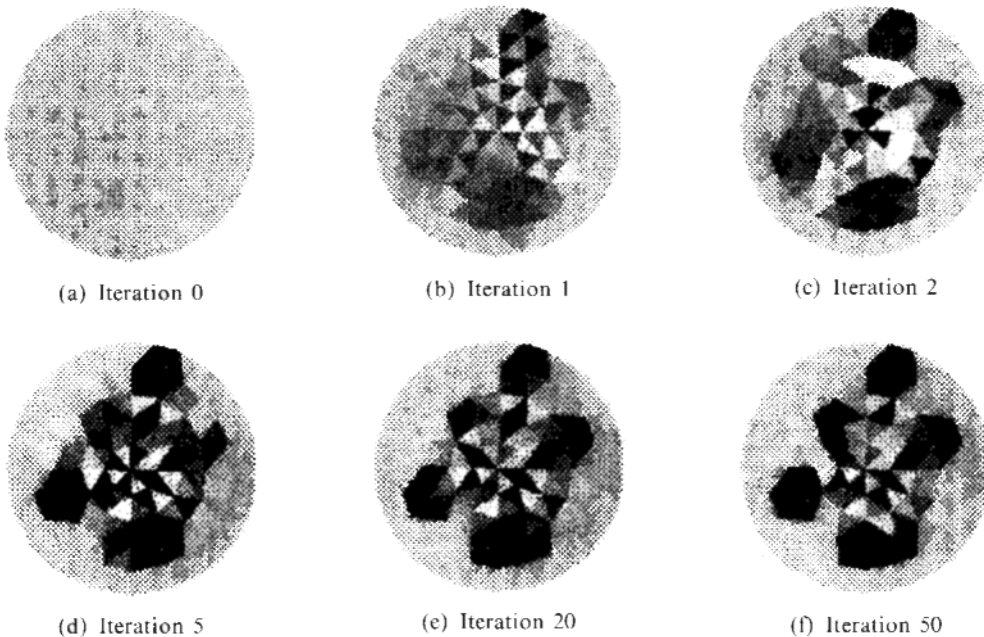
Figure 5 shows the reconstructed images by the conventional iNR method without mesh grouping for the sample target objects (e. g. bubbles) shown in Fig. 1. Even though the target seems to be simple, the iNR failed to reconstruct the target

image correctly. In Fig. 5, we may roughly estimate the profile and the location of the target after only a few iterations, e. g. five iterations. However, further iterations don't show much improvement. Even after 50 iterations as shown in Fig. 5 (f), there still remain considerable amount of errors in the reconstructed image. This kind of poor convergency is a very typical problem in the NR-type reconstruction algorithms in the EIT. In

**Table 1** Summary of the image reconstruction shown in Fig. 6 with mesh grouping

Mesh Group	No. of meshes in Base Group	No. of meshes in Object Group	No. of meshes in Adjust Group	No. of unknown variables in iNR	CPU time* [sec/iter]
0	0	0	152	152	5.19
1st	66	0	86	87	1.92
2nd	86	0	66	67	1.29
3rd	91	19	42	44	0.74
4th	110	26	16	18	0.29

\*) : CPU time per iteration in the iNR on Pentium PC (166MHz)



**Fig. 5** Reconstructed images by iNR without mesh grouping for the bubbles in Fig. 1.

the meanwhile, we can significantly improve the iNR's convergency by adopting the proposed mesh grouping method as follows.

In order to apply the mesh grouping method, we stopped the initial iNR process after five iterations. Figure 6(d) shows the image that is the

same one in Fig. 5(d), and Fig. 6(e) shows the first Fuzzy-GA classification result using the previous iNR iterations results. As shown in Table 1, it should be noted that 66 meshes among 152 ones are grouped to BaseGroup but none to ObjectGroup yet. The remains (darker regions in

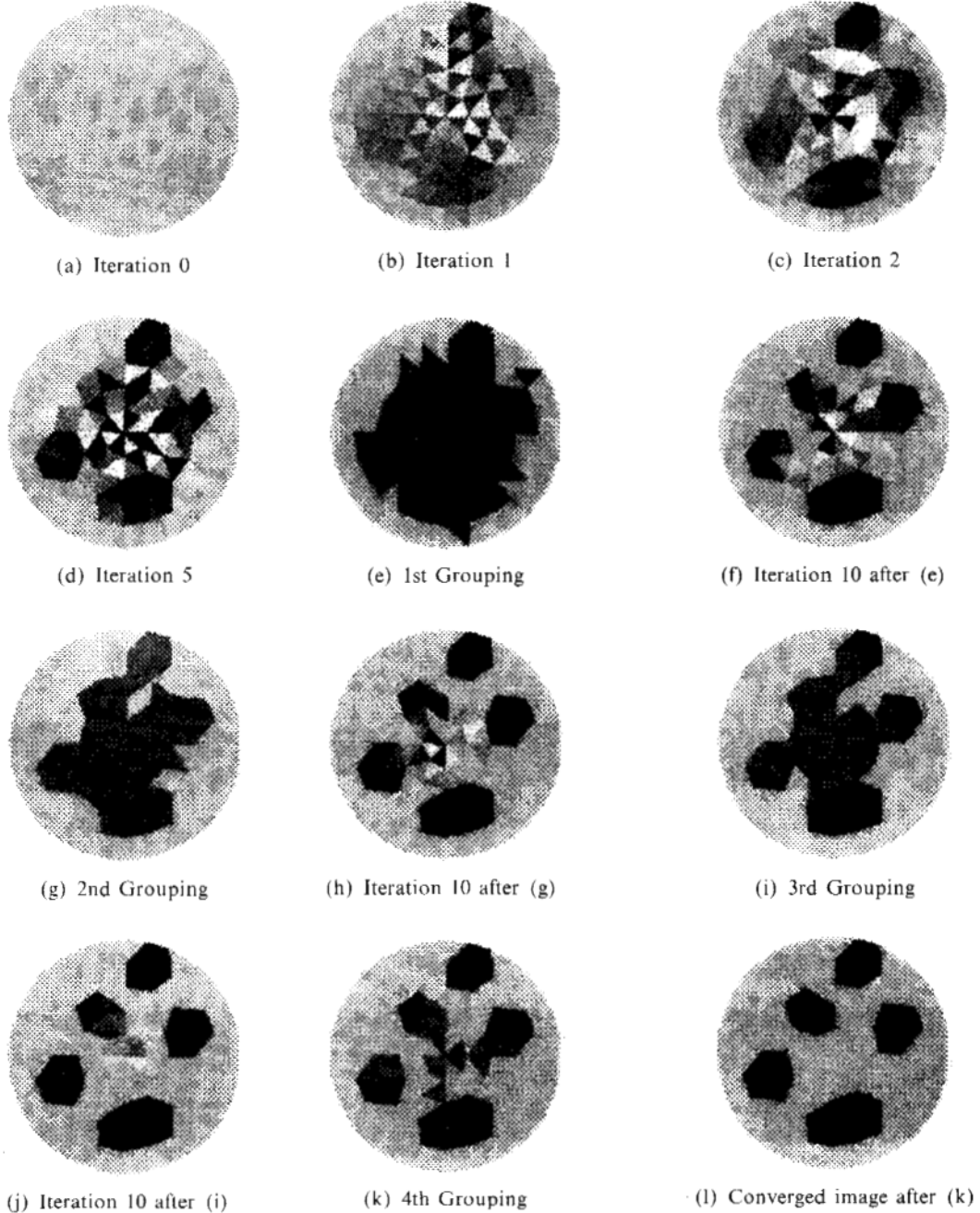


Fig. 6 Reconstructed images by iNR with mesh grouping for the bubbles in Fig. 1.



Fig. 6(e)) correspond to AdjustGroup. The number of unknowns is reduced to 87 and the iteration time is saved by 60% approximately at the next iNR iterations. Using the mesh grouping in Fig. 6(e), we restarted the second set of iNR iterations and obtained the image in Fig. 6(f) after 10 more iterations in iNR. Then we stopped again and applied the second fuzzy-GA classification to obtain the mesh grouping in Fig. 6(g). In Fig 6(i), after the third grouping, it should be noted that some meshes are now grouped to ObjectGroup and the BaseGroup becomes larger than in Fig. 6(g), so the AdjustGroup is reduced. Repeating these procedures, we obtain the final image in Fig. 6(l). The final image converges to the true one with the squared error sum  $\phi(\rho)$  less than  $10^{-7}$ .

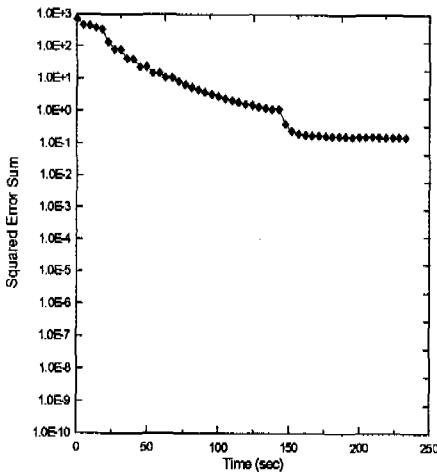
**4.2 Improvement on ill-posedness**

Figure 7 shows how the values of the objective function in Eq. (1) have changed during the image reconstruction shown in Figs. 5 and 6. Please be notified that the x-axis scales are different from each other in Fig. 7(a) and (b). Table 1 shows how the adaptive mesh grouping method has reduced not only the number of unknown variables but also the computation time in iNR iteration.

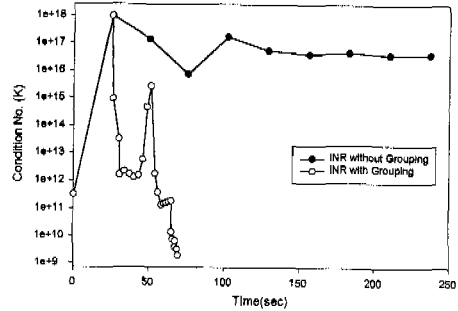
Usually, a matrix is called ill-conditioned when its condition number is very large. Figure 8

shows the changes of the condition number of the Hessian matrix  $H$  defined by Eq. (8). As can be seen in the figure, when mesh grouping is not applied, the iNR could not decrease the condition number further up to 50 iterations. On the contrary, the proposed mesh grouping method helps the iNR decrease the condition number significantly or mitigate the ill-conditioning phenomenon through out the repeated mesh grouping. Comparing this figure with Fig. 7, we can find that the proposed mesh grouping method helps to decrease the condition number of the Hessian matrix and improve the convergence characteristics, which eventually results in a great reduction in the total reconstruction time.

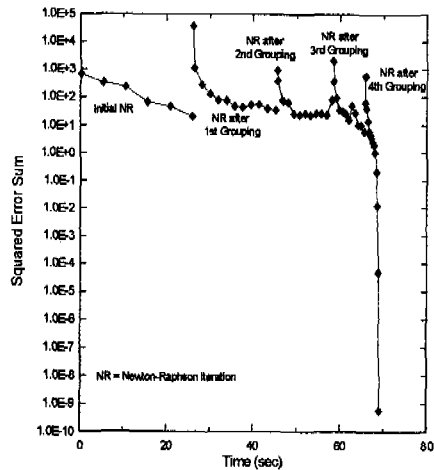
Table 2 shows several target (e. g. bubble) images which may be encountered in the two-phase flow fields. All these images were recon-



(a) Without Grouping



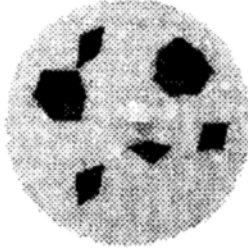
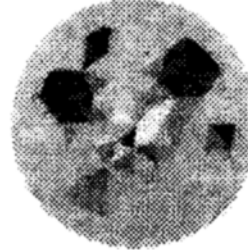
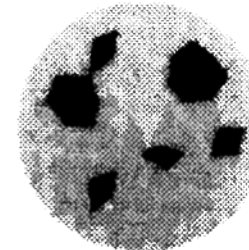
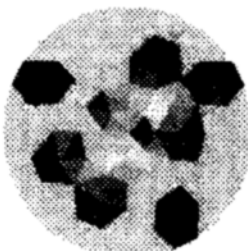

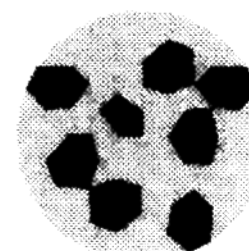
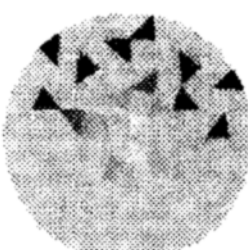
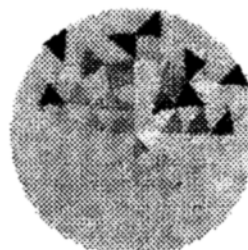
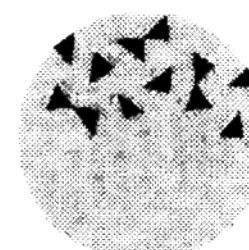
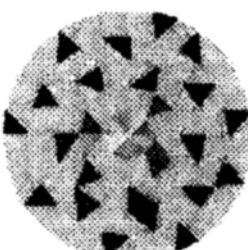
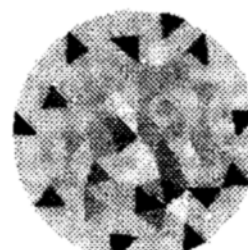
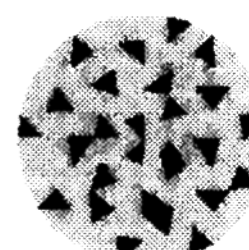
**Fig. 8** Condition numbers during the iterations in Figs. 5 and 6



(b) With Grouping

**Fig. 7** Values of the objective function in Eq. (1) for images shown in Figs. 5 and 6.

**Table 2** Summary of case studies for various bubbles

Case No.	Reconstructed Images				True Image
	with mesh grouping*		without mesh grouping		
	sec**	error $\phi(\rho)$	sec**	error $\phi(\rho)$	
1					
	7.41	$1.53 \times 10^1$	165.49	$9.70 \times 10^{-1}$	
2					
	28.29	$5.37 \times 10^0$	171.97	$4.38 \times 10^{-2}$	
3					
	50.20	$1.15 \times 10^1$	162.03	$2.96 \times 10^{-1}$	
4					
	65.47	$9.13 \times 10^0$	167.91	$4.05 \times 10^{-1}$	

\*) For all the cases above, the reconstructed images have converged to the true ones with  $\phi(\rho) < 10^{-7}$  within 5~10 seconds after the intermediate results shown above when the mesh grouping is applied.

\*\*\*) Elapsed CPU time on Pentium PC (166MHz)

structed easily with the squared error sum  $\phi(\rho)$  less than  $10^{-7}$  using the proposed mesh grouping method. On the contrary, the iNR algorithm without mesh grouping has failed to reconstruct any of these images correctly.

## 5. Conclusions

The EIT technology, which has been firstly proposed for the medical application, seems to have several advantages when it is applied to the two-phase flow measurements. First of all, it is a non-invasive measurement technique and its measuring speed is very fast. Even though this kind of potential ability of the EIT, several problems must be resolved in advance for its real application. One of the major problems is the rapid increase in the image reconstruction time with poor convergency as the spatial resolution increases. In this work, it is found that the iNR method which has been accepted to have a sound theoretical background also can not be free from this kind of problem. In other words, it is very difficult to visualize the bubble images by using the conventional EIT reconstruction method like the iNR method because the bubble visualization via the EIT is a highly nonlinear and ill-posed inverse problem.

We developed an adaptive mesh grouping method based on fuzzy-GA algorithm for the two-phase flow visualization based upon the EIT technique. When combined with iNR, it helps us decrease the condition number of the Hessian matrix thus get more improved solutions at the subsequent iNR iterations. Owing to the better conditioning by the repeated mesh groupings, we can eventually obtain the converged solution within a reasonable computation time with the personal computer for several noise free computer simulation test cases. The quality of the reconstructed images is also highly improved compared with the conventional iNR results.

We limited the implementation of the proposed mesh grouping algorithm to a system with two representative resistivity values. This would be a reasonable assumption for the two-phase flow fields. We are now working on increasing the

number of groups in order to extend the EIT to the multi-phase flow fields. This will require us to divide the ObjectGroup into several subgroups with multi-level representative resistivity values.

A study on the stability of the proposed algorithm in the presence of measurement and modeling errors has not been completed yet. However, we think that the stability will also be improved due to the better conditioning of the Hessian matrix as the mesh grouping increases the effective mesh size.

## Acknowledgment

This work has been supported in part by Electrical Engineering & Science Research Institute grant, 98-061 which is funded by Korea Electric Power Corporation.

## References

- Boone, K., Barber, D. and Brown, B., 1997, "Imaging with electricity : Report of the European concerted action on impedance tomography," *J. Med. Eng. & Tech.*, Vol. 21, pp. 201 ~232.
- Cheney, M., Isaacson, D., Newell, J. C., Simske, S. and Goble, J., 1990, "NOSER : An algorithm for solving the inverse conductivity problem," *Int. J. Imaging Syst. and Technol.*, Vol. 2, pp. 66 ~75.
- Cho, K. H., Woo, E. J. and Ko, S. T., 1997, "Fast static image reconstruction using adaptive mesh grouping method in EIT," *Proc. 19th Int. Conf. IEEE/EMBS*, Chicago, Oct. 30-Nov. 2, pp. 441 ~444.
- Dickin, F. and Yang, M., 1996, "Electrical resistance tomography for process application," *Meas. Sci. Technol.* Vol. 7, pp. 247~260.
- Elkow, K. J. and Rezkallar, K. S., 1996, "Void fraction measurements in gas-liquid flows using capacitance sensor," *Meas. Sci. Technol.* Vol. 7, pp. 1153~1163.
- Glidewell M. and Ng, K. T., 1995, "Anatomically constrained electrical impedance tomography for anisotropic bodies via a two-step approach," *IEEE Trans. Med. Imaging*, Vol. 14,

pp. 498~503.

Goldberg, D. E., 1989, *Genetic Algorithms in Search, Optimization and Machine Learning*, Addison-Wesley, New York.

Hua, P., Webster, J. G. and Tompkins, W. J., 1987, "Effect of the measurement method on noise handling and image quality of EIT imaging," *Proc. Annu. Int. Conf. IEEE Engineering in Medicine and Biology Society*, pp. 1429~1430.

Hua, P., Tompkins W. J. and Webster, J. G., 1988, "A regularised electrical impedance tomography reconstruction algorithm," *Clin. Phys. Physiol. Meas.* Vol. 9, Suppl. A, pp. 137~141.

Isaacson, D., 1986, "Distinguishability of conductivities by electric current computed tomography," *IEEE Trans. Medical Imaging*, MI-5, pp. 91~95.

Murai, T. and Kagawa, Y., 1985, "Electrical impedance computed tomography based on a finite element model," *IEEE Trans. Biomed. Eng.*, BME-32, pp. 177~184

Ovacik, L. Lin, J. -T. and Jones, O. C., 1997a, "Progress in electrical impedance imaging of binary media : 1 : Analytical and numerical methods," *1997 OECD/CSNI Specialists Meeting on Advanced Instrumentation*, Santa Babara, CA, pp. 17~20.

Ovacik, L. and Jones, O. C., 1997b, "Progress in electrical impedance imaging of binary media : 2 : Experimental developments and results," *1997 OECD/CSNI Specialists Meeting on Advanced Instrumentation*, Santa Babara, CA, pp. 17~20.

Paulsen, K. D., Meaney, P. M., Moskowitz, M. J. and Sullivan Jr., J. M., 1995, "A dual mesh scheme for finite element based reconstruction algorithm," *IEEE Trans. Med. Imaging*, Vol. 14, pp. 504~514.

Shollenberger, K. A., Torczynski, J. R., Adkins, D. R. O'Hernm T. J. and Jackson. N. B.

1997, "Gamma-densitometry tomography of gas holdup spatial distribution in industrial-scale bubble columns," *Chem. Eng. Sci.* Vol. 52, pp. 2037~2048.

Vassallo, P. F., Trabold, T. A., Moore, W. E. and Kirouac, G. J., 1993, "Measurement of velocities in gas-liquid two-phase flow using laser doppler velocimetry," *Exp. Fluids* Vol. 15, 227~236.

Webster, J. G. (ed), 1990, *Electrical Impedance Tomography*, Adam Hilger, Bristol.

Woo, E. J., 1990, *Finite Element Method and Reconstruction Algorithms in Electrical Impedance Tomography*, PhD Thesis, Dept. of Electrical and Computer Eng., Univ. Wisconsin Madison.

Woo, E. J., Hua, P., Webster, J. G. and Tompkins, W. J., 1992, "Measuring lung resistivity using electrical impedance tomography," *IEEE Trans. Biomed. Eng.*, Vol. 39, pp. 756~760.

Woo, E. J., Hua, P., Webster, J. G. and Tompkins, W. J., 1993, "A robust image reconstruction algorithm and its parallel implementation in electrical impedance tomography," *IEEE Trans. Med. Imaging*, Vol. 12, pp. 137~146.

Woo, E. J., Hua, P., Webster, J. G. and Tompkins, W. J., 1994, "Finite element method in electrical impedance tomography," *Med. & Biol. Eng. & Comput.*, Vol. 32, pp. 530~536.

Xu, L., Han, Y., Xu, L. A. and Yang, J., 1997, "Application of ultrasonic tomography to monitoring gas/liquid flow," *Chem. Eng. Sci.*, Vol. 52, pp. 2171~2183.

Yorkey, T., 1986, *Comparing reconstruction methods for electrical impedance tomography*, PhD Thesis, Dept. of Electrical and Computer Eng., Univ. Wisconsin, Madison.

Zimmermann, H. J., 1985, *Fuzzy Set Theory and Its Applications*, Kluwer Academic, Boston.